Electrosynthesis of poly(2,5-dimercapto-1,3,4-thiadiazole) films and their composites with gold nanoparticles at a polarised liquid|liquid interface

Marco F. Suárez-Herrera, [a,b,*] Alonso Gamero-Quijano [a,c,d] and Micheál D. Scanlon[a,c,e*]

[a] The Bernal Institute, University of Limerick (UL), Limerick V94 T9PX, Ireland.

[b] Departamento De Química, Facultad De Ciencias, Universidad Nacional De Colombia, Cra 30 # 45-03, Edificio 451, Bogotá, Colombia.

[c] Department of Chemical Sciences, School of Natural Sciences, University of Limerick (UL), Limerick V94 T9PX, Ireland.

[d] Department of Physical Chemistry, University of Alicante (UA), E-03080, Alicante, Spain.

[e] The Advanced Materials and Bioengineering Research (AMBER) Centre, CRANN Institute, Trinity College Dublin (TCD), Dublin 2 D02 PN40, Ireland

Corresponding authors:

*E-mail: mfsuarezh@unal.edu.co

*E-mail: micheal.scanlon@ul.ie

Abstract

The organosulfur compound 2,5-dimercapto-1,3,4-thiadiazole (DMcT) finds widespread applications in batteries, lubricant fluids, heavy metal ion sensors, waste-water purification and as a biocide. In this article, we demonstrate the untapped versatility inherent to using biphasic systems for electrosynthesis by showcasing several successful approaches to the electrosynthesis of poly(DMcT) films at a polarised interface between two immiscible electrolyte solutions (ITIES) by cyclic voltammetry (CV) cycling using either I_2, Hg^{2+} or O_2 as the oxidising agents. AC voltammetry is demonstrated as an effective *in situ* method to monitor poly(DMcT) film formation by I_2 or Hg^{2+} as a function of the aqueous electrolyte anion and pH. DMcT is further shown to act as a binder molecule to promote interfacial gold nanoparticle (AuNP) assembly into floating films at an immiscible liquid|liquid (L|L) interface. Exploiting the electrocatalysis of DMcT oxidation by O_2 in the presence of adsorbed interfacial AuNPs yields AuNP/poly(DMcT) composite films. Raman spectroscopy suggests the latter were a coordination polymer of poly(DMcT) with AuNPs and surface enhanced Raman spectroscopy (SERS) active. The dielectric nature of the poly(DMcT) films suppresses the capacitance at the ITIES, yet the AuNP/poly(DMcT) films show a very high interfacial capacitance, with an ability to efficiently adsorb cations. Thus, these films open opportunities to selectively modulate the interfacial capacitance, potentially forming the basis of novel “soft” capacitors at a polarised L|L interface.

1. Introduction

The redox and chelating properties of the organosulfur compound 2,5-dimercapto-1,3,4-thiadiazole (DMcT) enable versatile applications for electrochemical energy storage in lithium ion batteries as a cathode active material [1–5], as a multifunctional additive in lubricating oils and greases [6,7], as a biocide [8], and as a chelating agent in heavy metal ion sensors [9] and absorbent materials for waste-water purification [10–13].

Maiti *et al.* reported the selective binding affinity of DMcT on metallic nanoparticle (NP) surfaces, specifically silver (Ag) and gold (Au) NP surfaces, *via* the ring nitrogen atom and the thiocarbonyl or thiadiazole ring sulfur atom (see Scheme 1 for the molecular structure of DMcT) [14]. However, to our knowledge, this selective binding affinity has yet to be exploited to promote the assembly or (electro)synthesis of novel colloidal AgNP or AuNP supramolecular nanostructures or composites for potential applications in redox electrocatalysis, nanoplasmonic sensors, electrovariable optics, sieve membranes, supercapacitors, *etc*. [15–18].

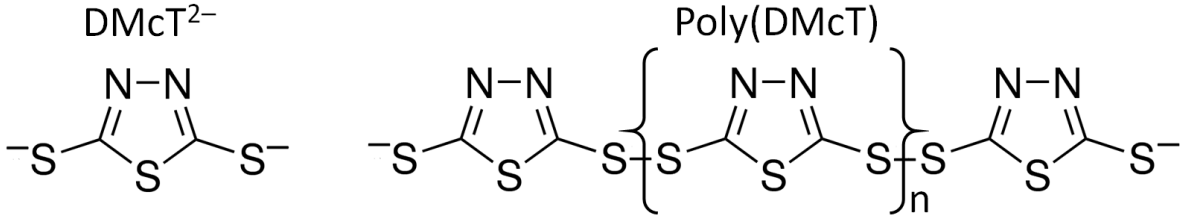

Scheme 1. Chemical structures of the ionic form of 2,5-dimercapto-1,3,4-thiadiazole ($DMcT^{2-}$) and poly(DMcT).

Electrochemistry at the interface between two immiscible electrolyte solutions (ITIES) opens opportunities to electrosynthesis materials that are inaccessible by traditional routes employing bulk chemical synthesis in a single phase or electrosynthesis on conductive solid electrode surfaces [19]. The use of two solvents of different polarity facilitates interfacial reactions between redox couples with incompatible solubilities. For example, we recently demonstrated the electrosynthesis of conducting poly(3,4-ethylenedioxythiophene) (PEDOT) thin films at an immiscible aqueous|α,α,α-trifluorotoluene interface using an aqueous oxidant (Ce^{4+}) and organic monomer (EDOT) [20]. The free-standing nature of the resulting thin films easily permits their transfer to any solid substrate for *ex situ* characterisation or device applications.

Solid (nano)materials, such as molybdenum disulfide or graphene flakes, carbon nanotubes (CNTs) or metallic NPs, initially suspended in either the aqueous or organic phase may be entrapped in significant quantities at a liquid|liquid (L|L) interface by simply shaking/sonicating the biphasic system [21–24] or polarising the L|L interface (*e.g.*, by repetitive cyclic voltammetry (CV) cycling) [25]. The adsorbed (nano)materials may electrocatalytically enhance the kinetics of interfacial electron transfer (IET) between redox couples in opposite phases by providing a conductive electrical "short-cut" of low-overpotential and/or a catalytic surface for both species to adsorb onto and react [16,25,26]. In this manner, unique composite material thin films may then be prepared by electrosynthesising a second material, such as a polymer, around the adsorbed (nano)materials. Further control over the driving force for IET with adsorbed AuNPs is provided by tuning their Fermi level through the adsorption of aqueous anions upon external polarisation of the ITIES [25,27]. In this regard, we designed a biphasic system to oxidise organic soluble elemental sulfur (S_8) by dissolved oxygen (O_2) under ambient conditions with a AuNP film as an interfacial catalyst [25]. This biphasic approach overcame the incompatible solubilities of the hydrophobic reactants (O_2 and S_8) and hydrophilic products (H^+, SO_3^{2-}, SO_4^{2-}, *etc.*) [25].

Depending on its protonation state, DMcT is either aqueous or organic soluble. Herein, we demonstrate the electrochemically-driven oxidation of (i) deprotonated aqueous soluble $DMcT^{2-}$ by organic soluble iodine (I_2) and (ii) protonated organic soluble H_2DMcT by aqueous mercurous cations (Hg^{2+}), forming an interfacial film of poly(DMcT) in both instances. We further show that dissolved O_2 can oxidise DMcT in the presence of adsorbed interfacial AuNPs that provide a catalytic surface onto which O_2 and DMcT can adsorb and form chemical bonds. As discussed *vide infra*, the resulting AuNP/poly(DMcT) composite displayed a high interfacial capacitance at the polarised L|L interface and an ability to efficiently adsorb cations, opening potential opportunities to design novel "soft" capacitors at polarised L|L interfaces.

2. Results and Discussion

2.1 Oxidation of $DMcT^{2-}$ by I_2. Li *et al.* reported that I_2 oxidises H_2DMcT monomers in a homogeneous ethanol solution to oligomers in high yield [10]. Taking into account the poor solubility of I_2 in water, Electrochemical Cell 1 (Fig. 1a) was designed such that aqueous $DMcT^{2-}$ was oxidised by organic I_2 at a polarised L|L interface. Repetitive CV cycling led to the electrosynthesis of an interfacial poly(DMcT) film as seen in the optical image in Fig. 1b taken after 70 CV cycles. Further images are provided in Fig. S1 clearly showing that

electrosynthesis takes place mainly at the polarised L|L interface and a well-defined poly(DMcT) film is formed.

CV experiments were carried out using either LiCl or Li_2SO_4 as the aqueous electrolyte (Fig. 1c,d and Fig. S2). In both cases, two reversible diffusion-controlled charge transfer responses were observed with half-wave potentials at ca. 0 and +0.150 V, respectively, in the absence of $DMcT^{2-}$. Subsequently, the larger charge transfer response at ca. 0 V increased in magnitude with CV cycling in the presence of $DMcT^{2-}$. During interfacial electrosynthesis, I_3^- is generated *in situ* as, upon oxidation of $DMcT^{2-}$, I_2 is reduced to I^- in the organic phase and then further reacts with I_2 to form I_3^- (Reactions (1) and (2)):

$$n\mathrm{DMcT}^{2-}{}_{(\mathrm{aq})} + m\mathrm{I}_{2\,(\mathrm{org})} \rightarrow \mathrm{poly(DMcT)}n_{\,(\mathrm{int})} + 2m\mathrm{I}^-{}_{(\mathrm{org})} \quad (1)$$

$$2m\mathrm{I}^-{}_{(\mathrm{org})} + 2m\mathrm{I}_{2\,(\mathrm{org})} \rightarrow 2m\mathrm{I}_3^-{}_{(\mathrm{org})} \quad (2)$$

where (aq) and (org) denote the aqueous and organic sides of the ITIES and (int) denotes the L|L interface. As detailed in a series of control experiments (Fig. S3), the charge transfer response at ca. 0 V is attributed to the reversible ion transfer of I_3^- and provides a clear signal to follow the progress of the interfacial electrosynthesis of poly(DMcT). The other smaller charge transfer response at ca. +0.150 V is tentatively assigned to the ion transfer of hypoiodite (IO^-), which forms when I_2 reacts with water (Reaction (3)):

$$\mathrm{I}_{2\,(\mathrm{org})} + \mathrm{H_2O} \rightarrow \mathrm{IO}^-{}_{(\mathrm{org})} + 2\mathrm{H}^+{}_{(\mathrm{aq})} + \mathrm{I}^-{}_{(\mathrm{org})} \quad (3)$$

Control experiments with $DMcT^{2-}$ in the aqueous phase in the absence of organic I_2 further clarified that the charge transfer response at ca. +0.150 V was not due to $DMcT^{2-}$, as the standard ion transfer potential of $DMcT^{2-}$ lies outside the negative extreme of the polarisable potential window (PPW) at the ITIES (Fig. S4).

The CVs in Fig. 1c,d show a *pseudo*-steady state current at potentials positive of the standard ion transfer potential of I_3^-. Higher steady-state currents were obtained in the presence of Li_2SO_4 than LiCl (Fig. 1d), indicating that the polymerisation reaction proceeds faster with LiCl as less I_3^- is detected by CV at the L|L interface. I_3^- is an intermediary species that further reacts with $DMcT^{2-}$ upon transfer to the organic phase. Thus, if the steady-state concentration of I_3^- at the interface is low, it means that its rate of reaction with $DMcT^{2-}$ is high. Fig. 1d also suggests that I_2Cl^- is transferred at the same potential as I_3^- as the magnitude of the charge transfer between –0.1 and +0.1 V in the absence of $DcMT^{2-}$ (dashed CVs) is higher in the presence of LiCl than Li_2SO_4.

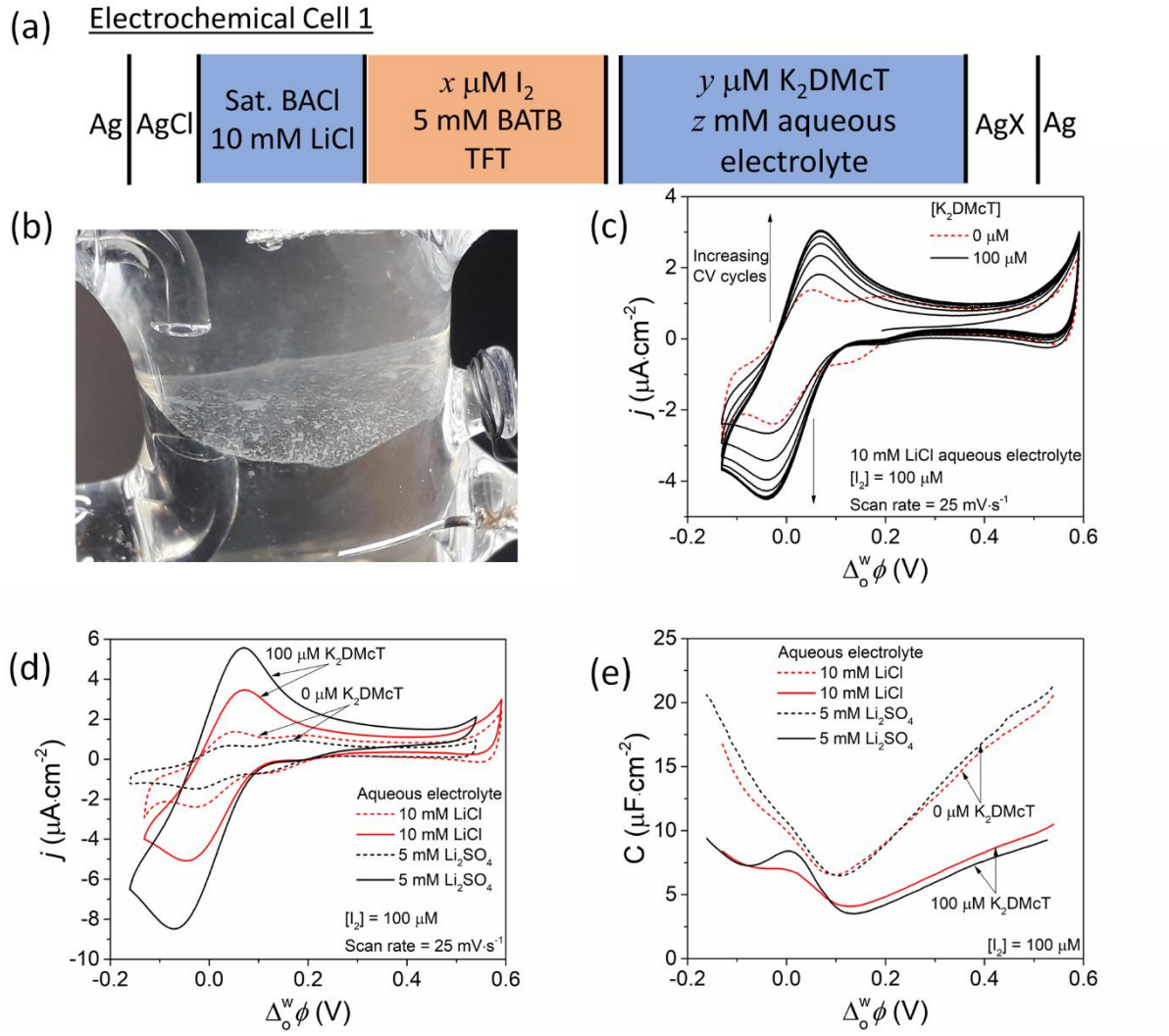

Figure 1. Oxidation of $DMcT^{2-}$ by I_2 to form a poly(DMcT) interfacial film. (a) Schematic representation of Electrochemical Cell 1 to oxidise aqueous solubilised $DMcT^{2-}$ by organic I_2 at a polarised liquid|liquid (L|L) interface. **(b)** Optical image of poly(DMcT) electrosynthesised using a 5 mM Li_2SO_4 aqueous electrolyte, after 70 CV cycles with 100 μM aqueous K_2DMcT and 100 μM organic I_2. CVs were obtained at a scan rate of 25 $mV \cdot s^{-1}$. **(c)** Repetitive cyclic voltammetry (CV) cycles to electrosynthesis poly(DMcT) when the aqueous electrolyte was 10 mM LiCl in the absence and presence of aqueous K_2DMcT. CV cycles 1 to 10 are shown. Comparison of **(d)** CVs and **(e)** differential capacitance curves in the presence and absence of K_2DMcT when the aqueous phase was either 10 mM LiCl or 5 mM Li_2SO_4. Data is shown for CV cycle 10 and differential capacitance curves taken after 50 and 70 CV cycles for LiCl and Li_2SO_4 aqueous electrolytes, respectively. Differential capacitance measurements were taken using a voltage excitation frequency of 80 Hz. All electrochemical experiments were carried out using Electrochemical Cell 1 under aerobic, ambient conditions.

The electrosynthesis of poly(DMcT) at the ITIES leads to a significant decrease in the differential capacitance measured by AC voltammetry compared to that at a bare L|L interface (Fig. 1e). Differential capacitance curves were taken after 50 and 70 CV cycles for LiCl and Li_2SO_4 aqueous electrolytes, respectively. The most appropriate frequency to study the differential capacitance using AC voltammetry without the interference of the ion transfer of I_3^- was identified as 80 Hz, irrespective of the aqueous electrolyte used, as described in Fig. S3e. Decreases in the interfacial capacitance have previously been reported for ITIES functionalised with carbonaceous materials, with Toth *et al.* suggesting that the physical presence of graphene suppresses capillary waves which locally roughen the L|L interface [28]. Another explanation is that the relative dielectric permittivity of graphene is low, with an effective dielectric constant (ε) reported in the range of 3–16 [29]. Similarly, poly(DMcT) has an electrically insulating nature [2] and this leads to a reduction of the electrical permittivity of the L|L interface and a proportional reduction of the interfacial capacitance. The potential of zero charge (PZC) shifted positively after electrosynthesis of poly(DMcT), indicating that the poly(DMcT) film has an overall net anionic charge, which is consistent with the negative charges present at the extremes of each oligomer in the film (*i.e.*, the first and last monomer) as shown in Scheme 1.

2.2 Oxidation of H_2DMcT by Hg^{2+}. The influence of the aqueous electrolyte anion (Cl^- *versus* SO_4^{2-}) and the aqueous phase pH on the electrosynthesis of the poly(DMcT) film using a Hg^{2+} oxidant was investigated. Electrochemical Cell 2 (Fig. 2a) was designed such that organic H_2DMcT was oxidised by aqueous Hg^{2+} at a polarised L|L interface. Control CV experiments in the absence of organic H_2DMcT revealed that the negative end of the PPW shortens in the presence of aqueous $HgCl_2$ in 5 mM H_2SO_4 (Fig. S5a). As reviewed by Powell *et al.* [30], the chemical speciation of aqueous Hg^{2+} varies as a function of the aqueous anion (Cl^- or SO_4^{2-} herein) concentration and the pH. Thus, Hg^{2+} can facilitate the transfer of aqueous anions to the organic phase at less negative Galvani potentials by forming complexes such as $HgCl_4^{2-}$ in the presence of LiCl or $Hg(SO_4)_2^{2-}$ in the presence of H_2SO_4 or Li_2SO_4. Also, differential capacitance curves taken after 50 CV cycles in the absence of organic H_2DMcT were broadly unchanged in the presence of increasing concentrations of $HgCl_2$ (Fig. S5b), with a slight positive shift of the PZC suggesting the adsorption of an anion at the L|L interface (such as $HgCl_4^{2-}$).

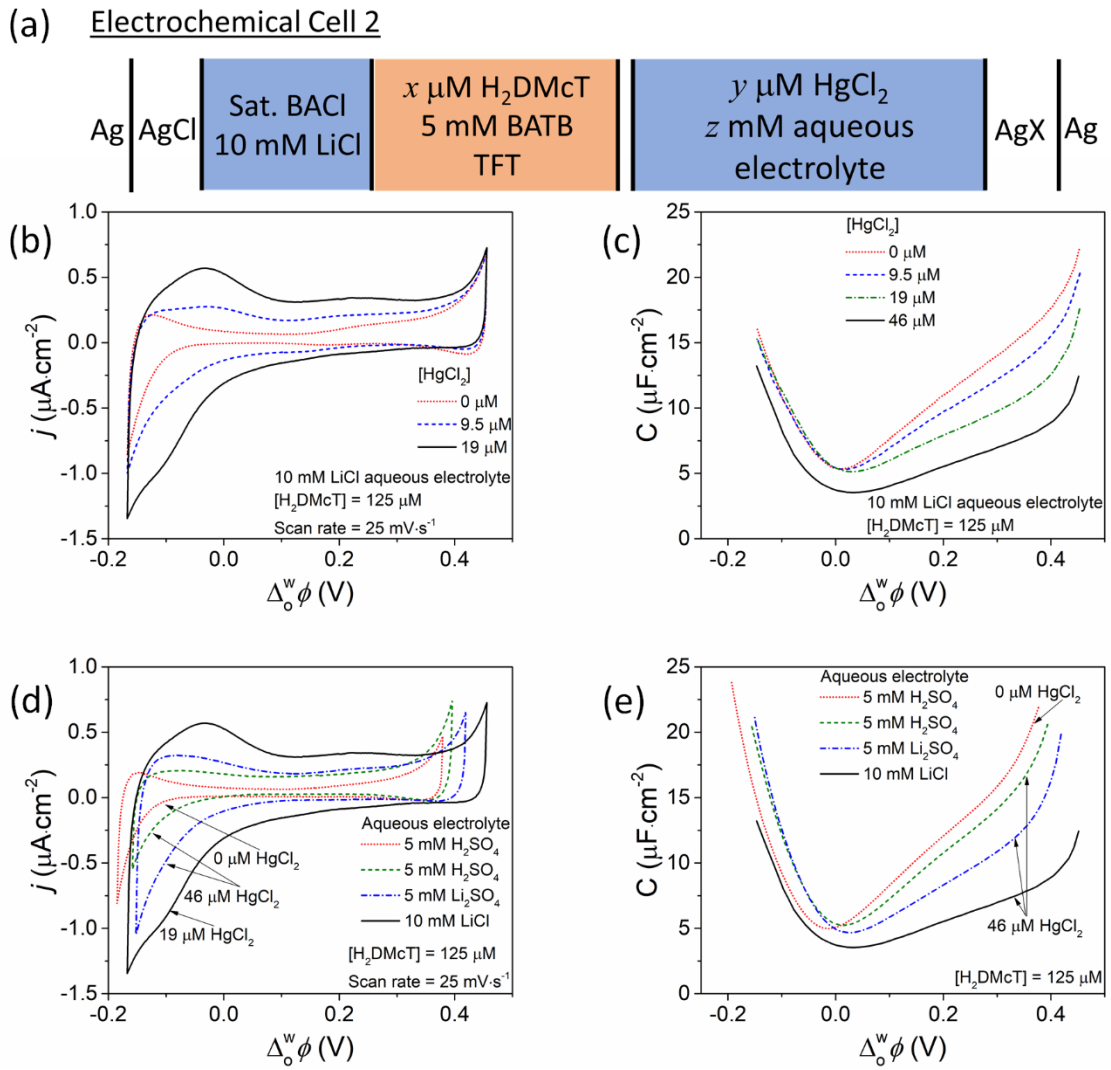

Figure 2. Oxidation of H_2DMcT by Hg^{2+} to form a poly(DMcT) interfacial film. (a) Schematic representation of Electrochemical Cell 2 to oxidise organic solubilised H_2DMcT by aqueous Hg^{2+} at a polarised L|L interface. **(b)** CVs and **(c)** differential capacitance curves obtained in the absence and presence of increasing concentrations of aqueous $HgCl_2$, with 10 mM LiCl aqueous electrolyte and 125 μM organic H_2DMcT. **(d)** CVs and **(e)** differential capacitance curves obtained in the absence and presence of $HgCl_2$, with either 5 mM H_2SO_4, 5 mM Li_2SO_4 or 10 mM LiCl aqueous electrolyte and 125 μM organic H_2DMcT. CVs were obtained at a scan rate of 25 mV·s^{-1}. CVs shown were for CV cycle 5 with LiCl aqueous electrolyte and CV cycle 50 with H_2SO_4 and Li_2SO_4 aqueous electrolytes. Differential capacitance measurements were taken using a voltage excitation frequency of 80 Hz. Differential capacitance curves shown were obtained after 5 CV cycles with LiCl aqueous electrolyte and 50 CV cycles with H_2SO_4 and Li_2SO_4 aqueous electrolytes. All electrochemical experiments were carried out using Electrochemical Cell 2 under aerobic, ambient conditions.

CV and differential capacitance experiments using Electrochemical Cell 2 in the presence of organic H_2DMcT and increasing concentrations of aqueous $HgCl_2$ were carried out using 10 mM LiCl (Fig. 2b,c), 5 mM H_2SO_4 (Fig. S5c,d) and 5 mM Li_2SO_4 (Fig. S5e,f) aqueous electrolytes, respectively. For each aqueous electrolyte investigated, an increase in positive and negative current was measured across the full PPW by CV. Also, fully in-line with earlier observations using I_2 as the oxidant, differential capacitance curves revealed a positive shift of the PZC and a decrease in the interfacial capacitance during poly(DMcT) interfacial electrosynthesis. Each of these trends increased in magnitude as the aqueous $HgCl_2$ concentration increased.

We propose that the electrosynthesis of poly(DMcT) is initiated at negative Galvani potentials by ion transfer of either $HgCl_4^{2-}$ (or $Hg(SO_4)_2^{2-}$) to the organic phase (Reaction (4)). The ensuring homogeneous polymerisation reaction on the organic side of the ITIES leads to the formation of DMcT oligomers, that adsorb at the L|L interface ultimately leading to the nucleation and growth of a poly(DMcT) film. While the polymerisation reaction is homogeneous, it should be clarified that polymerisation only occurs in close vicinity to the mixed solvent interfacial region and not in the bulk organic phase. During the electrosynthesis, Cl^- (or SO_4^{2-}) anions and protons are continuously released into the organic phase (Reaction (5) and subsequently undergo spontaneous ion transfer to the aqueous phase, generating positive and negative currents, respectively, across the full PPW (Reactions (6) and (7)). No such increases in current were observed for the control CVs in the absence of organic H_2DMcT (Fig. S5a).

$$\mathrm{HgCl_4}^{2-}{}_{(aq)} \overset{IT}{\rightarrow} \mathrm{HgCl_4}^{2-}{}_{(org)} \qquad (4)$$

$$n\mathrm{H_2DMcT}_{(org)} + m\mathrm{HgCl_4}^{2-}{}_{(org)} \rightarrow \mathrm{poly(DMcT)}n_{\,(int)} + m\mathrm{Hg}^{2+}{}_{(org)} + m\mathrm{Cl}^-{}_{(org)} + 2n\mathrm{H}^+{}_{(org)} \qquad (5)$$

$$\mathrm{Cl}^-{}_{(org)} \overset{IT}{\rightarrow} \mathrm{Cl}^-{}_{(aq)} \qquad (6)$$

Comparisons of CVs (Fig. 2d) and differential capacitance curves (Fig. 2e) obtained using Electrochemical Cell 2 in the presence of organic H_2DMcT and aqueous $HgCl_2$ using 10 mM LiCl, 5 mM H_2SO_4, and 5 mM Li_2SO_4 aqueous electrolytes, respectively, demonstrated that Cl^- anions and less acidic aqueous electrolyte enhance the kinetics of poly(DMcT) interfacial electrosynthesis. The positive and negative ionic currents detected by CV (Fig. 2d) and the drop in interfacial capacitance (Fig. 2e) with LiCl exceeded those seen with Li_2SO_4

and H_2SO_4 aqueous electrolytes. These enhanced kinetics with Cl^- were attributed to the greater ease (less negative Galvani potentials) with which $HgCl_4^{2-}$ transfers to the organic phase, compared with the analogous $Hg(SO_4)_2^{2-}$ species, and associated with the additional peak-shaped features seen only in CVs with LiCl at negative Galvani potentials. Furthermore, the positive and negative ionic currents detected by CV (Fig. 2d) and the drop in interfacial capacitance (Fig. 2e) with Li_2SO_4 exceeded that seen with H_2SO_4 aqueous electrolyte. At less acidic conditions, H_2DMcT may deprotonate to form $DMcT^{2-}$ at the L|L interface (the p*K*a of H_2DMcT is 5.77 calculated using ChemAxon® software). In this regard, Suarez-Herrera *et al.* previously demonstrated that the kinetics of oxidation are faster for the deprotonated anionic $DMcT^{2-}$ species than H_2DMcT [31].

2.3 Electrocatalytic oxidation of H_2DMcT by O_2 in the presence of colloidal gold nanoparticles (AuNPs). The adsorption of O_2 on a macroscopic gold surface is unlikely [32], making gold a bad catalyst for oxidation reactions. However, AuNPs [33] and nanoporous gold [34] are good catalysts for many oxidation reactions [35]. Previously, we studied the electrocatalysis of elemental sulfur oxidation by O_2 in the presence of adsorbed AuNPs at the ITIES [25]. Herein, the ability to prepare AuNP/poly(DMcT) composite films is demonstrated by exploiting the electrocatalysis of H_2DMcT oxidation by O_2 in the presence of adsorbed AuNPs at the ITIES. Colloidal AuNPs initially suspended in the aqueous phase may be entrapped at the L|L interface, forming AuNP interfacial films, by simply shaking/sonicating the biphasic system [21–24] or polarising the L|L interface (*e.g.*, by repetitive CV cycling) [25].

Dithiols, such as DMcT, can act as binder molecules bridging two AuNPs, thereby promoting interfacial AuNP agglomeration or assembly. As a proof-of-concept to explore this effect, simple "shake-flask" experiments were designed (see biphasic cell in Fig. 3a) with an organic solution containing H_2DMcT contacted with an aqueous suspension of phosphate buffered saline (PSB)-stabilised colloidal AuNPs. Previously, we have shown that while PBS-stabilised AuNP suspensions remain stable in the bulk aqueous phase, if these AuNPs come into proximity with a L|L interface they lose their ionic solvation shells, induced by the electric field at the interface and/or by changes of the local solvent polarity [25]. Thus, PBS gives the dynamic freedom necessary to avoid agglomeration in the bulk aqueous phase but, at the same time, facilitates a change of the AuNPs ionic and solvation cloud at the L|L interface with PBS being displaced by DMcT molecules. After vigorous shaking, followed by a settling time for phase separation, a blue AuNP/poly(DMcT) composite film formed stably at both the air|aqueous and aqueous|organic interfaces (Fig. 3b). Also, some flakes extended across the bulk aqueous phase between these two interfaces. Scanning electron microscopy (SEM) images

obtained by depositing the AuNP/poly(DMcT) films on a silicon wafer by the horizontal dipping method show that the AuNPs assembled into a 2D interfacial film (Fig. 3c,d).

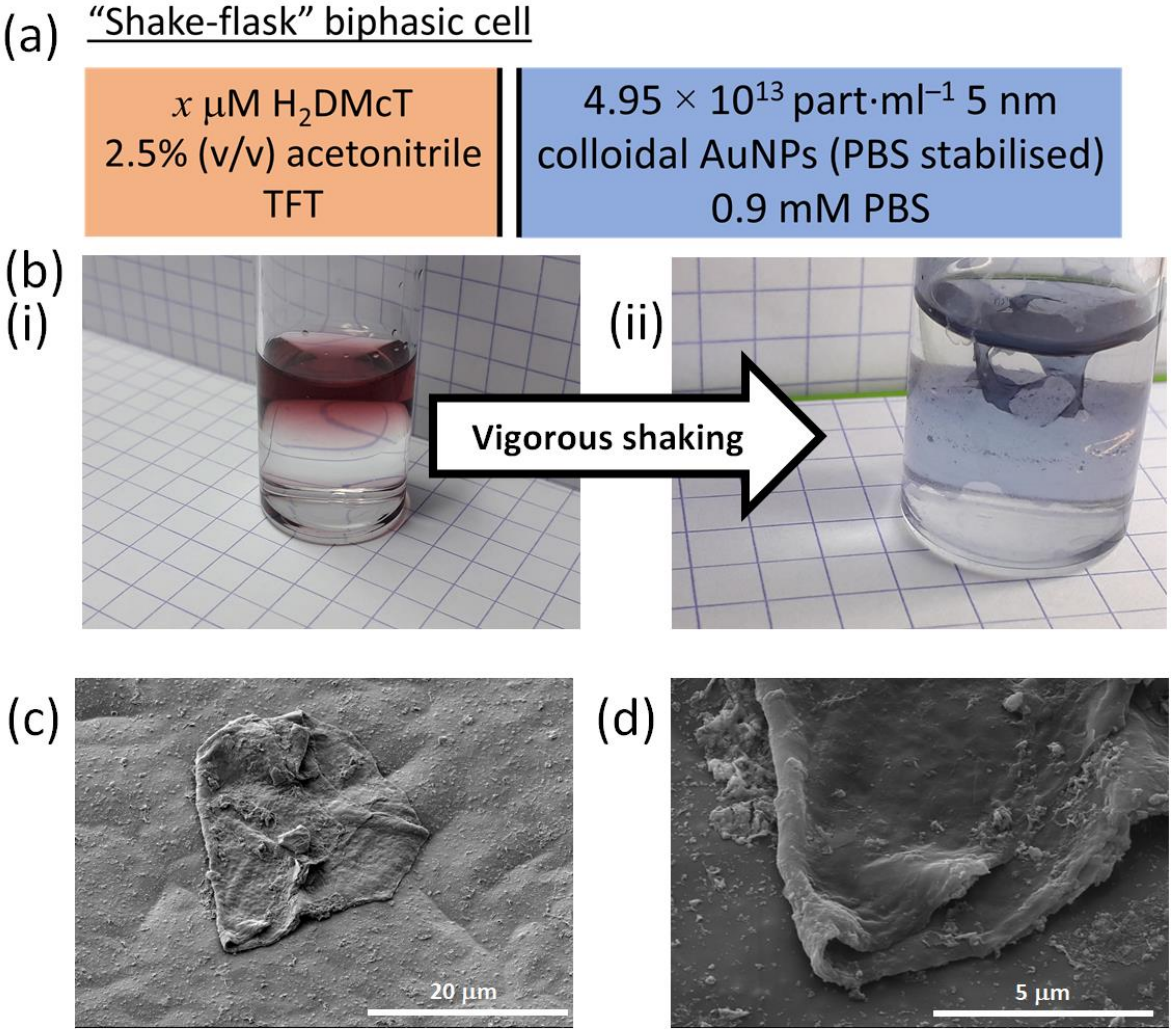

Figure 3. Inducing AuNP/poly(DMcT) interfacial film formation using the "shake-flask" approach. **(a)** Schematic representation of the "shake-flask" biphasic cell to oxidise 330 μM organic solubilised H_2DMcT by O_2 (dissolved in both the aqueous and organic phases) in the presence of a AuNP electrocatalyst. **(b)** Optical images of a vial containing the biphasic system described **(i)** before and **(ii)** after shaking for ca. 30s, followed by waiting for 120 s to allow phase separation. **(c, d)** Scanning electron microscopy (SEM) images of the AuNP/poly(DMcT) film shown in (b) after immobilisation on a silicon wafer substrate by the horizontal dipping method.

Initial control experiments using the four-electrode electrochemical cell explored the uncatalysed oxidation of organic H_2DMcT by O_2 (dissolved in both the aqueous and organic

phases) in the absence of AuNPs at the polarised L|L interface (Fig. S6). With repetitive CV cycling, the currents associated with the ion transfer of Li^+ and Cl^- aqueous electrolyte ions at the positive and negative ends of the PPW, respectively, decreased slowly. This was attributed to the slow oxidation of H_2DMcT by O_2, producing a poly(DMcT) film at the L|L interface. As poly(DMcT) is a dielectric material as discussed *vide supra*, it both reduces the interfacial capacitance and blocks the movement of ions through the L|L interface. The film of poly(DMcT) formed after 100 CV cycles was not readily observable by eye or recoverable from the L|L interface.

Further control experiments studied the formation of a AuNP film at the polarised L|L interface in the absence of organic H_2DMcT by repetitive CV cycling in the presence of PBS-stabilised colloidal AuNPs as described in Electrochemical Cell 3 (Fig. 4a). As the AuNP film formed at the L|L interface with successive CV cycles, the capacitance increased at negative Galvani potentials (Fig. 4b). Previously, Younan *et al.* showed that the capacitance of the L|L interface increases in the presence of an adsorbed monolayer of citrate coated AuNPs and attributed this to an increase of the interfacial charge density or by an increase of the interfacial corrugation [36]. In Fig. 4b, the increase of the interfacial charge density is related to the adsorption of Cl^- anions on the AuNPs adsorbed at the interface [37].

AuNP/poly(DMcT) films were formed using Electrochemical Cell 3 by repetitive CV cycling when PBS-stabilised AuNPs were present in the aqueous phase and H_2DMcT in the organic phase (Fig 4c). Scanning the CVs to the limits of the PPW (–0.240 to +0.510 V) led to an increase in positive and negative current across the full PPW. This observation is fully in-line with that seen for the oxidation of H_2DMcT by Hg^{2+} (see CVs in Fig. 2 and Fig. S5) and attributed to the transfer of protons (released during the polymerisation of H_2DMcT) and $(DMcT)_n^{2-}$ oligomers across the polarised L|L interface. Furthermore, the production of OH^- anions during H_2DMcT oxidation is likely (this mechanism will be detailed fully *vide infra*). Thus, all of these ions undergo spontaneous ion transfer in different directions according to the applied Galvani potential, thereby increasing the currents along the whole PPW.

If the CVs were scanned within a narrower potential range (–0.090 to +0.410 V), not approaching the positive and negative limits of the PPW, then no AuNP/poly(DMcT) interfacial film formed and no increases in current across the full PPW were recorded. Potential cycling using a wide PPW was required to enhance the catalytic cycle as at negative Galvani potentials the adsorption of O_2 on the AuNPs is favoured, while at positive Galvani potentials the polymerisation of $DMcT^{2-}$ was more likely. Optical images show a free-floating AuNP/poly(DMcT) interfacial film before (Fig. 4d(i)) and after (Fig. 4d(ii)) all remaining

colloidal AuNPs in the bulk aqueous phase were extracted by thoroughly rinsing with a colloidal AuNP-free aqueous electrolyte solution (*e.g.*, 10 mM LiCl). The aqueous-facing side of the AuNP/poly(DMcT) film was dark blue, but the underlying organic-facing side was white (see Fig. S7). This indicates that AuNP agglomeration was faster in the presence of H_2DMcT and poly(DMcT) asymmetrically decorated the organic-facing side of the AuNP interfacial film.

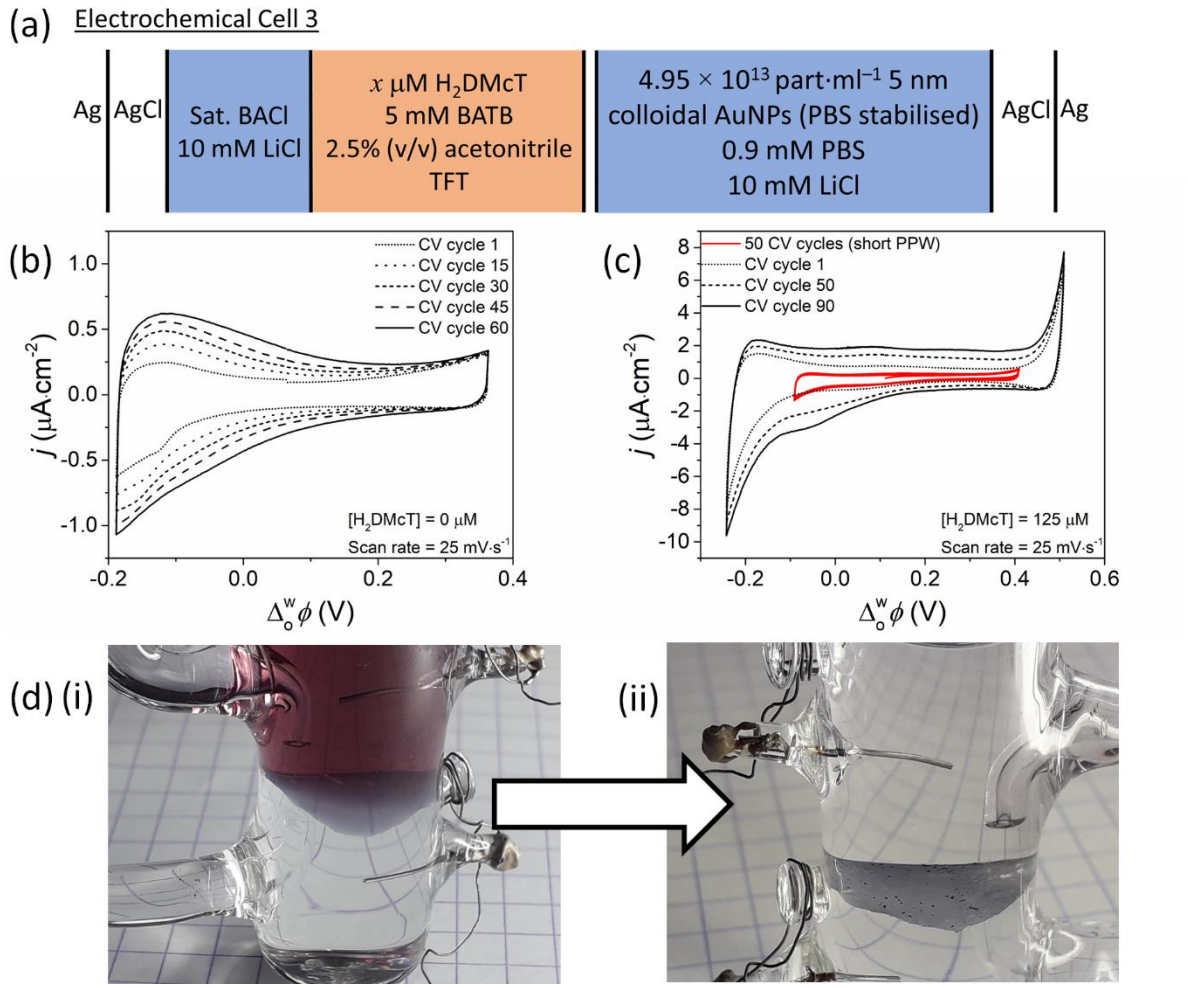

Figure 4. Electrocatalysis of the oxidation of H_2DMcT by O_2 in the presence of colloidal gold nanoparticles (AuNPs) to form a AuNP/poly(DMcT) composite interfacial film. (a) Schematic representation of Electrochemical Cell 3 to oxidise organic solubilised H_2DMcT by O_2 (dissolved in both the aqueous and organic phases) in the presence of a AuNP electrocatalyst at a polarised L|L interface. Repetitive CV cycles **(b)** in the absence and **(c)** in the presence of 125 μM organic H_2DMcT. CVs were obtained at a scan rate of 25 $mV \cdot s^{-1}$ using Electrochemical Cell 3 under aerobic, ambient conditions. **(d) (i)** Optical image of a four-electrode electrochemical cell with formation of a AuNP/poly(DMcT) interfacial film using

Electrochemical Cell 3 with 125 μM organic H_2DMcT after 100 CV cycles. **(ii)** Optical image of the aqueous-facing side of a free-floating AuNP/poly(DMcT) interfacial film after all remaining colloidal AuNPs in the bulk aqueous phase were extracted by thoroughly rinsing with a colloidal AuNP-free aqueous electrolyte solution (*e.g.*, 10 mM LiCl).

2.4 Electrochemical analysis of free-floating AuNP and AuNP/poly(DMcT) interfacial films. The electrochemical properties of free-floating AuNP and AuNP/poly(DMcT) interfacial films were studied using Electrochemical Cells 4a and 4b, respectively (Fig. 5a), once all remaining colloidal AuNPs in the bulk aqueous phase were extracted by thoroughly rinsing with a 10 mM LiCl aqueous electrolyte solution (see images in Fig.4d(ii) and Fig. 5b). All CVs were recorded at different scan rates and with *iR* compensation applied.

The adsorption of aqueous Cl^- anions on the AuNP interfacial film gave rise to a well-defined reversible signal between –0.2 V and +0.2 V (Fig. 5c), as we outlined in detail recently [25]. Simulations show that the adsorption of Cl^- can be reasonably described by a Frumkin model (red CV in Fig. 5c), with a repulsive interaction factor of 11.6 kJ mol^{-1}, total surface charge 8 mC cm^{-2}, and electron transfer rate constant 5 s^{-1}. Compared to the CVs obtained with the AuNP interfacial film, the voltammetry of the AuNP/poly(DMcT) film was significantly different (Fig. 5d), with higher currents and a greater asymmetry between the CV peaks recorded between –0.2 V and +0.2 V as a function of the scan rate (Fig. S8).

The adsorption and reduction of O_2 is promoted on negatively charged AuNPs and through proton-coupled electron transfer reactions [25]. Charge transfer from the support to the AuNPs is typically needed to enhance the O_2 reduction reaction (ORR) on gold [38] and it has been reported that O_2 anions (O_2^-) preferentially adsorb on AuNPs compared with O_2 molecules [39]. Thus, we propose that the signal N_1 in Fig. 5d is related to the following reactions:

$$Cl^-_{(aq)} \rightarrow Cl^-_{(ad)} \quad (8)$$

$$O_2 + Cl^-_{(ad)} \rightarrow O_{2\,(ad)}^- + Cl_{(ad)} \quad (9)$$

$$O_{2\,(ad)}^- + H_2O_{(ad)} \rightarrow HO_{2\,(ad)}^- + OH_{(ad)} \quad (10)$$

$$HO_{2\,(ad)}^- + H_2O_{(ad)} \rightarrow 2OH_{(ad)} + OH^-_{(ad)} \quad (11)$$

$$OH^-_{(ad)} + Cl_{(ad)} \rightarrow OH_{(ad)} + Cl^-_{(ad)} \quad (12)$$

where (ad) means adsorbed on the interfacial AuNPs' surface. Furthermore, the signal P_1 is related to the desorption of Cl^-:

$$Cl^-_{(ad)} \rightarrow Cl^-_{(aq)} \qquad (13)$$

We also propose that the irreversible signal P_2 in Fig. 5d is related to the oxidation of H_2DMcT, as at positive Galvani potentials the oxidised AuNPs have a low enough Fermi level to allow oxidation reactions [25]. Thus, the first step of the electrocatalytic oxidation of H_2DMcT to poly(DMcT) by O_2 in the presence of interfacial AuNPs can be described by reaction (14):

$$H_2DMcT_{(ad,oil)} + 2OH_{(ad,aq)} \rightarrow (HDMcT)_{2(ad)} + 2OH^-_{(aq)} + 2H^+_{(org)} \qquad (14)$$

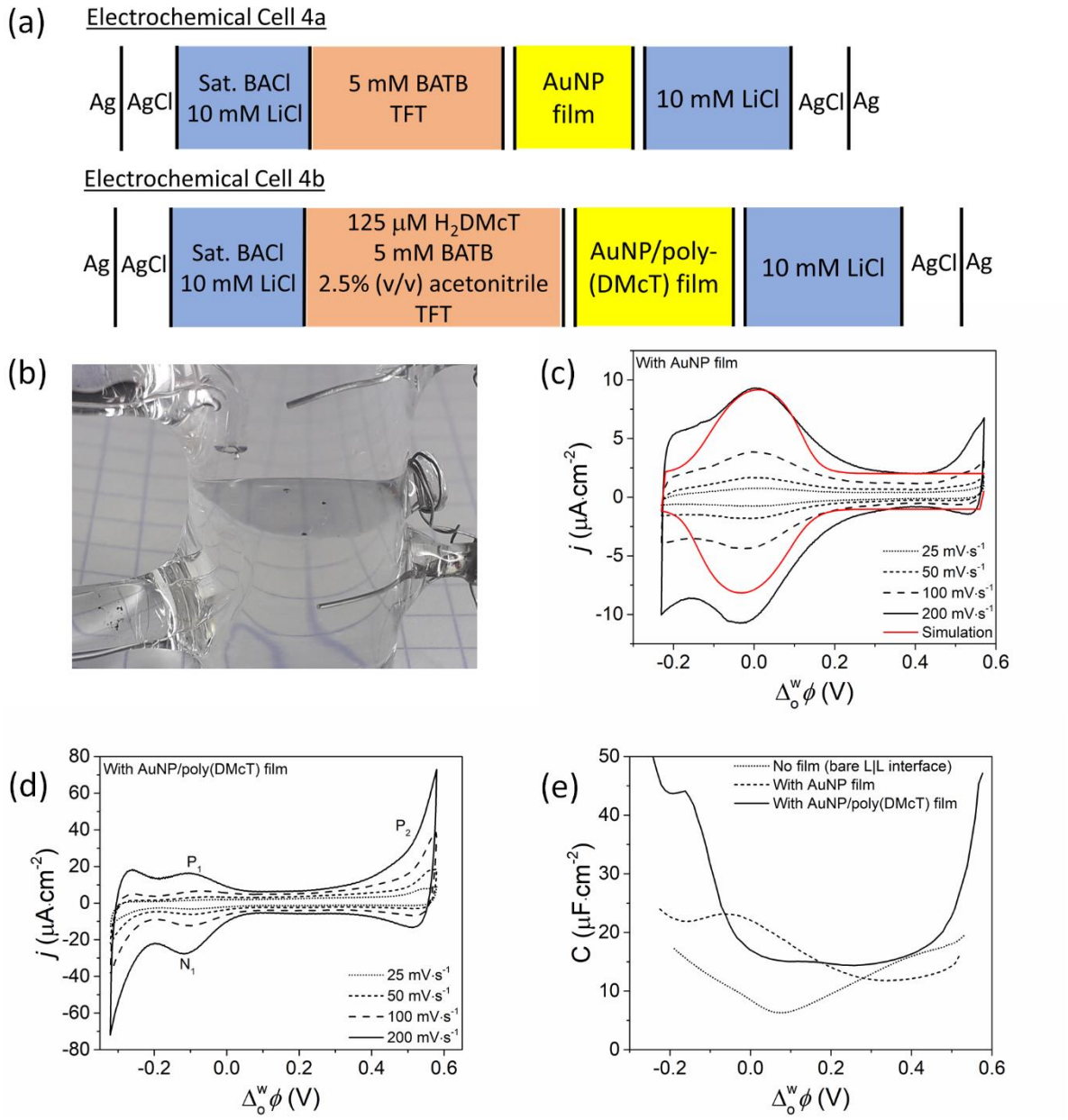

Figure 5. Electrochemical analysis of free-floating AuNP and AuNP/poly(DMcT) interfacial films. (a) Schematic representation of Electrochemical Cells 4a and 4b with pre-

formed AuNP and AuNP/poly(DMcT) interfacial films, respectively, and the aqueous suspension of colloidal AuNPs replaced by a 10 mM LiCl aqueous electrolyte. **(b)** Optical image of the free-floating AuNP interfacial film. The corresponding image of the AuNP/poly(DMcT) interfacial film is shown in Figure 4d(ii). CVs at different scan rates and with *iR* compensation for the biphasic systems described in **(c)** Electrochemical Cell 4a and **(d)** Electrochemical Cell 4b. In (c), a computer simulation of the CV at 200 mV s^{-1} (red CV) using a Frumkin isotherm is shown (repulsive interaction factor of 11.6 kJ mol^{-1}, total surface charge 8 μC cm^{-2}, electron transfer rate constant 5 s^{-1}). **(e)** Comparison of differential capacitance measurements taken using a voltage excitation frequency of 80 Hz at a bare L|L interface (using the same configuration as described in Electrochemical Cells 4(a) without the AuNP film present), and in the presence of either a AuNP or AuNP/poly(DMcT) interfacial film.

Analysis of the peak current *versus* scan rate for the CVs in Fig. 5c, d is presented in Fig. S8. In the presence of the AuNP interfacial film (Fig. 5c and Fig. S8a), the adsorption peaks due to Cl^- anions were not completely symmetrical (contrary to expectation), possibly due to the presence of some background currents (capacitive, parasitic and/or ionic faradaic currents) as the ITIES is away from equilibrium upon formation [40]. In the presence of the AuNP/poly(DMcT) interfacial film, a linear trend between the peak current and scan rate (Fig. S8b) shows that the signals P_1 and N_1 in Fig. 5d were related to kinetically controlled processes at the ITIES due to adsorption of ions on the AuNPs and/or the polarised L|L interface. The observation that the signal between 0 and -0.2 V was highly asymmetric (peak $N_1 > P_1$) suggests that the adsorption rate of Cl^- (reaction (8)) is higher than its desorption rate (reaction 12), and that the irreversible reduction of O_2 to $OH_{(ad)}$ take place between 0 and –0.2 V.

Differential capacitance curves were compared for a bare L|L interface, “free” of solid materials, and in the presence of either a AuNP or AuNP/poly(DMcT) interfacial film (Fig. 5e). The capacitance increased at negative Galvani potentials in the presence of both the AuNP and AuNP/poly(DMcT) interfacial films (Fig. 5e). These observations were due to the increase of the interfacial charge density related to the adsorption of Cl^- anions on the AuNPs in each interfacial film [37], as discussed *vide supra* for the analysis of the CVs in Fig. 4b recorded during the electrochemically-induced assembly of the AuNP interfacial films. Regarding the AuNP/poly(DMcT) interfacial film, DMcT facilitates the aggregation of AuNPs at the L|L interface, thereby providing more AuNPs for the Cl^- anions to adsorb onto at the L|L interface. However, the presence of poly(DMcT) also inhibits Cl^- anion adsorption on the AuNPs in the

composite as the polymer donates negative charge to the AuNPs. The latter is reflected in the more negative onset Galvani potential in Fig. 5e for substantial Cl^- adsorption on the AuNPs in the AuNP/poly(DMcT) film (at ca. 0 V) than the AuNP film (at ca. +0.25 V). Furthermore, the adsorption of cations at positive potentials (> ca. 0.4 V) also increases in the presence of the AuNP/poly(DMcT) interfacial film. This ability of the AuNP/poly(DMcT) to efficiently adsorb cations may be exploited to build a capacitor with a specific capacitance at "soft" L|L interfaces. Electrical double-layer capacitors possess high power capabilities and long cycle life but have low energy densities. *Pseudo*-capacitors, or secondary batteries, store electrical energy *via* Faradaic processes with high energy density, but the power density, in general, is quite low. The ITIES will allow the design of energy storage devices with high electrical double-layer capacitance by using AuNP/poly(DMcT) films of variable thickness and, at the same time, high *pseudo*-capacitance by dissolving a hydrophobic reducing agent in the oil phase, *e.g.*, coenzyme Q10, and a hydrophilic oxidising agent in the aqueous phase, *e.g.*, Ce^{4+}, that can undergo reversible redox reactions.

2.5 Raman spectra of a AuNP/poly(DMcT) film. The interactions between the DMcT and AuNPs in the AuNP/poly(DMcT) films were analysed *ex situ* by confocal Raman spectroscopy at low and high vibrational frequencies (Fig. 6). The broad band at 204 cm^{-1} was attributed to Au-N stretching (Fig. 6a). This vibrational band only appears with high concentrations of DMcT and is only recorded due to a surface enhanced Raman spectroscopy (SERS) effect [14,41]. The sharp vibrational peak at 380 cm^{-1} was assigned to a S-Au bond, clearly showing the presence of metal-sulfur linkages (Fig. 6a). Notably, the presence of the C-S-C and ring Raman stretching modes at 660 and 1060 cm^{-1}, respectively, confirmed that the aromatic ring of DMcT was preserved during the interfacial electrosynthesis (Fig. 6b) [14]. The absence of bands centered at 917 (Fig. 6b) and 2490 cm^{-1} (Fig. S9) due to S-H stretching strongly suggested that DMcT (initially dissolved as H_2DMcT in the organic phase) was chemisorbed dissociatively on the gold surface by the rupture of both S-H bonds [41]. S-H-Au hydrogen bonding observed at 937 cm^{-1} (Fig. 6b) suggested a mixture of coordination species present in the AuNP/poly(DMcT) film. Pure poly(DMcT) has strong bands at 1380, 1084 and 643 cm^{-1} that can be assigned to the C=N stretch, N–N stretch and symmetric C–S–C stretch, respectively [11]. Fig. 6 shows that all of those signals are present in the AuNP/poly(DMcT) film but the signal related to the C=N and N–N stretches shift to lower values (1363 cm^{-1} and 1078 cm^{-1}) due to the SERS effect associated to the strong interaction between the polymer and AuNPs [41]. Overall, Raman spectroscopy strongly suggested the interfacial electrosynthesis of a coordination polymer of poly(DMcT) with AuNPs, a structure proposed

previously by Tiwari *et al.* [42] for their one-pot synthetic approach to preparing AuNP/poly(DMcT).

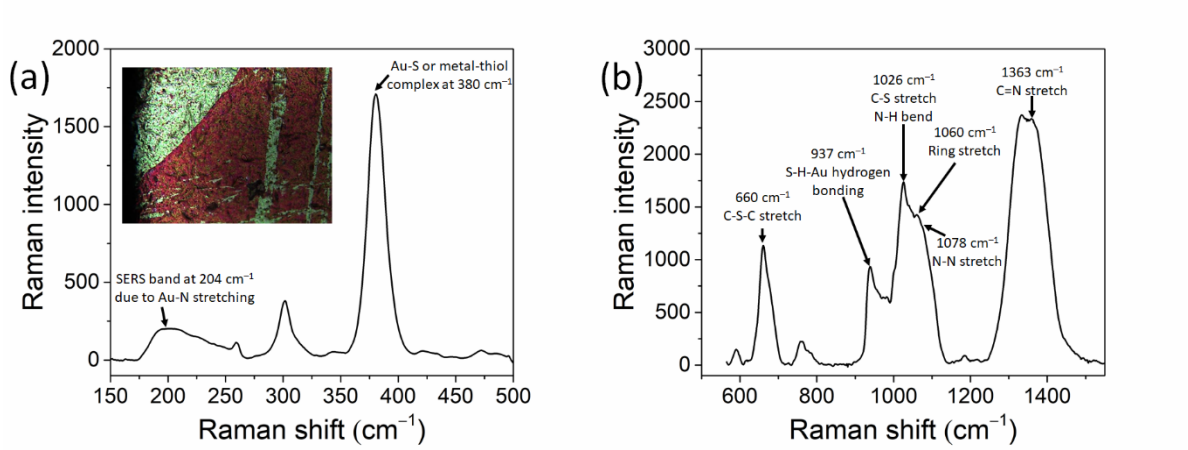

Figure 6. Raman spectra of a AuNP/poly(DMcT) film at **(a)** low and **(b)** high vibrational frequencies. The excitation laser wavelength was 785 nm. Inset in (a): optical micrograph of a AuNP/poly(DMcT) film immobilised on a silicon wafer substrate. The silicon wafer is green and the red/orange colour is the AuNP/poly(DMcT) film.

3. Conclusions

The electrosynthesis poly(DMcT) films at a polarised L|L interface by repetitive CV cycling was investigated firstly using organic soluble I_2 as the oxidant in combination with aqueous soluble $DMcT^{2-}$ and secondly using aqueous soluble Hg^{2+} as the oxidant with organic soluble H_2DMcT. AC voltammetry was demonstrated as an effective *in situ* technique to monitor the electrosynthesis of these interfacial thin films, that did not give well-defined ion or electron transfer signals within the available PPW. Significant decreases in the differential capacitance were measured compared to a bare L|L interface and attributed to the electrically insulating nature of poly(DMcT) that leads to a reduction of the electrical permittivity of the L|L interface. With I_2 as the organic oxidant, the interfacial electrosynthesis could also be followed by monitoring the well-defined and reversible ion transfer signal of I_3^- that was generated *in situ* upon oxidation of $DMcT^{2-}$. With Hg^{2+} as the aqueous oxidant, the kinetics of the interfacial electrosynthesis were dependent on the nature of the aqueous electrolyte anion and pH. Faster kinetics were observed with 10 mM LiCl than 5 mM Li_2SO_4, showing that Cl^- and SO_4^{2-} influenced the electrosynthetic reaction by facilitating the ion transfer of Hg^{2+} to the organic phase as either $HgCl_4^{2-}$ or $Hg(SO_4)_2^{2-}$, respectively. At less acidic conditions, H_2DMcT

may deprotonate to form $DMcT^{2-}$ at the L|L interface, and the kinetics of oxidation have previously been reported to be faster for $DMcT^{2-}$ than H_2DMcT.

DMcT is shown to promote interfacial AuNP agglomeration or assembly into stable films by acting as a binder molecule bridging two AuNPs. AuNP/poly(DMcT) films were subsequently electrosynthesised by exploiting the electrocatalysis of H_2DMcT oxidation by O_2 in the presence of adsorbed AuNPs at the ITIES. Raman spectroscopy strongly suggested the AuNP/poly(DMcT) film is SERS-active and a coordination polymer of poly(DMcT) with AuNPs. The poly(DMcT) and AuNP/poly(DMcT) films formed open opportunities to modulate the capacitance at a polarised L|L interface, potentially forming the basis of novel "soft" capacitors. As poly(DMcT) behaves as a dielectric material with a very low dielectric permittivity, the interfacial capacitance can be decreased upon its growth at the ITIES. By comparison, AuNP/poly(DMcT) shows a very high interfacial capacitance, with an ability to efficiently adsorb cations.

Finally, the work described herein demonstrates the outstanding versatility inherent to using polarised liquid|liquid interfaces for either catalysed or uncatalysed electrosynthesis of thin films, of either insulating or conducting materials (and their composites), and with total freedom to use either aqueous or organic soluble monomers.

Declaration of Competing Interest

The authors declare that they have no known competing financial interests or personal relationships that could have appeared to influence the work reported in this paper.

CRediT authorship contribution statement

Marco F. Suárez-Herrera: Data curation; conceptionalisation; investigation; methodology; writing original draft. **Alonso Gamero-Quijano:** Data curation; investigation; methodology; writing. **Micheál D. Scanlon:** Data curation; conceptionalisation; methodology; project administration; resources, writing – review & editing; funding acquisition.

Acknowledgements

M.D.S. acknowledges Science Foundation Ireland (SFI), under Grant No. 13/SIRG/2137 and the European Research Council through a Starting Grant (Agreement No. 716792). A.G.-Q. acknowledges funding received from an Irish Research Council (IRC) Government of Ireland Postdoctoral Fellowship Awards (Grant Numbers GOIPD/2018/252). M.F.S.-H. acknowledges

the “Universidad Nacional de Colombia” for allowing his sabbatical leave and the “Fundación Banco de la República” through the grant 4.562.

Keywords

Interface between two immiscible electrolyte solutions (ITIES); interfacial electrosynthesis; interfacial gold nanoparticle assembly; heterogeneous catalysis; AC voltammetry.

References

[1] J.M. Pope, T. Sato, E. Shoji, N. Oyama, K.C. White, D.A. Buttry, Organosulfur/Conducting Polymer Composite Cathodes, J. Electrochem. Soc. 149 (2002) A939. https://doi.org/10.1149/1.1482768.

[2] N. Oyama, Y. Kiya, O. Hatozaki, S. Morioka, H.D. Abruña, Dramatic Acceleration of Organosulfur Redox Behavior by Poly(3,4-ethylenedioxythiophene), Electrochem. Solid-State Lett. 6 (2003) 10–14. https://doi.org/10.1149/1.1621753.

[3] Y. Kiya, A. Iwata, T. Sarukawa, J.C. Henderson, H.D. Abruña, Poly[dithio-2,5-(1,3,4-thiadiazole)] (PDMcT)-poly(3,4-ethylenedioxythiophene) (PEDOT) composite cathode for high-energy lithium/lithium-ion rechargeable batteries, J. Power Sources. 173 (2007) 522–530. https://doi.org/10.1016/j.jpowsour.2007.04.086.

[4] G.G. Rodríguez-Calero, S. Conte, M.A. Lowe, J. Gao, Y. Kiya, J.C. Henderson, H.D. Abruña, Synthesis and characterization of poly-3,4-ethylenedioxythiophene/2,5-dimercapto-1,3,4-thiadiazole (PEDOT-DMcT) hybrids, Electrochim. Acta. 167 (2015) 55–60. https://doi.org/10.1016/j.electacta.2015.02.159.

[5] J. Gao, M.A. Lowe, S. Conte, S.E. Burkhardt, H.D. Abruña, Poly(2,5-dimercapto-1,3,4-thiadiazole) as a Cathode for Rechargeable Lithium Batteries with Dramatically Improved Performance, Chem. - A Eur. J. 18 (2012) 8521–8526. https://doi.org/10.1002/chem.201103535.

[6] A. V. Naletova, D. V. Davydov, V.N. Bakunin, Derivatives of 2,5-Dimercapto-1,3,4-Thiadiazole as Multifunctional Lubricant Additives, Chem. Technol. Fuels Oils. 57 (2021) 783–791. https://doi.org/10.1007/s10553-021-01307-x.

[7] J. Wang, J. Wang, C. Li, G. Zhao, X. Wang, A study of 2,5-dimercapto-1,3,4-thiadiazole derivatives as multifunctional additives in water-based hydraulic fluid, Ind. Lubr. Tribol. 66 (2014) 402–410. https://doi.org/10.1108/ilt-11-2011-0094.

[8] Ł. Popiołek, U. Kosikowska, M. Dobosz, A. Malm, Synthesis and antimicrobial properties of new thiosemicarbazide, 1,2,4-triazole, and 1,3,4-thiadiazole derivatives of sulfanylacetic acid, Phosphorus, Sulfur Silicon Relat. Elem. 187 (2012) 468–481. https://doi.org/10.1080/10426507.2011.625511.

[9] N. Vasimalai, G. Sheeba, S.A. John, Ultrasensitive fluorescence-quenched chemosensor for Hg(II) in aqueous solution based on mercaptothiadiazole capped silver nanoparticles, J. Hazard. Mater. 213–214 (2012) 193–199. https://doi.org/10.1016/j.jhazmat.2012.01.079.

[10] C. Li, S. Huang, C. Min, P. Du, Y. Xia, C. Yang, Q. Huang, Highly Productive Synthesis, Characterization, and Fluorescence and Heavy Metal Ion Adsorption Properties of Poly(2,5-dimercapto-1,3,4-thiadiazole) Nanosheets, Polymers (Basel). 10 (2017) 24. https://doi.org/10.3390/polym10010024. https://doi.org/10.3390/polym10010024.

[11] P. Tzvetkova, P. Vassileva, R. Nickolov, Modified silica gel with 5-amino-1,3,4-thiadiazole-2-thiol for heavy metal ions removal, J. Porous Mater. 17 (2010) 459–463. https://doi.org/10.1007/s10934-009-9308-1.

[12] L. Fu, S. Wang, G. Lin, L. Zhang, Q. Liu, J. Fang, C. Wei, G. Liu, Post-functionalization of UiO-66-NH2 by 2,5-Dimercapto-1,3,4-thiadiazole for the high efficient removal of Hg(II) in water, J. Hazard. Mater. 368 (2019) 42–51. https://doi.org/10.1016/j.jhazmat.2019.01.025.

[13] O. Olkhovyk, M. Jaroniec, Ordered mesoporous silicas with 2,5-dimercapto-1,3,4-thiadiazole ligand: High capacity adsorbents for mercury ions, Adsorption. 11 (2005) 205–214. https://doi.org/10.1007/s10450-005-5393-x.

[14] N. Maiti, R. Chadha, A. Das, S. Kapoor, Surface selective binding of 2,5-dimercapto-1,3,4-thiadiazole (DMTD) on silver and gold nanoparticles: A Raman and DFT study, RSC Adv. 6 (2016) 62529–62539. https://doi.org/10.1039/c6ra10404e.

[15] R. Dong, T. Zhang, X. Feng, Interface-Assisted Synthesis of 2D Materials: Trend and Challenges, Chem. Rev. 118 (2018) 6189–6325. https://doi.org/10.1021/acs.chemrev.8b00056.

[16] P. Peljo, M.D. Scanlon, A.J. Olaya, L. Rivier, E. Smirnov, H.H. Girault, Redox Electrocatalysis of Floating Nanoparticles: Determining Electrocatalytic Properties without the Influence of Solid Supports, J. Phys. Chem. Lett. 8 (2017) 3564–3575. https://doi.org/10.1021/acs.jpclett.7b00685.

[17] A.N.J. Rodgers, S.G. Booth, R.A.W. Dryfe, Particle deposition and catalysis at the

interface between two immiscible electrolyte solutions (ITIES): A mini-review, Electrochem. Commun. 47 (2014) 17–20. https://doi.org/10.1016/j.elecom.2014.07.009.

[18] W.H. Binder, Supramolecular assembly of nanoparticles at liquid-liquid interfaces, Angew. Chemie - Int. Ed. 44 (2005) 5172–5175. https://doi.org/10.1002/anie.200501220.

[19] A.J.G.G. Zarbin, Liquid–liquid interfaces: a unique and advantageous environment to prepare and process thin films of complex materials, Mater. Horizons. 8 (2021) 1409–1432. https://doi.org/10.1039/D0MH01676D.

[20] R.A. Lehane, A. Gamero-Quijano, S. Malijauskaite, A. Holzinger, M. Conroy, F. Laffir, A. Kumar, U. Bangert, K. McGourty, M.D. Scanlon, Electrosynthesis of Biocompatible Free-Standing PEDOT Thin Films at a Polarized Liquid|Liquid Interface, J. Am. Chem. Soc. 144 (2022) 4853–4862. https://doi.org/10.1021/jacs.1c12373.

[21] M.D. Scanlon, E. Smirnov, T.J. Stockmann, P. Peljo, Gold Nanofilms at Liquid-Liquid Interfaces: An Emerging Platform for Redox Electrocatalysis, Nanoplasmonic Sensors, and Electrovariable Optics, Chem. Rev. 118 (2018) 3722–3751. https://doi.org/10.1021/acs.chemrev.7b00595.

[22] H.A. Al Nasser, M.A. Bissett, R.A.W. Dryfe, The Modified Liquid-Liquid Interface: The Effect of an Interfacial Layer of MoS2 on Ion Transfer, ChemElectroChem. 8 (2021) 4445–4455. https://doi.org/10.1002/celc.202100820.

[23] E. Smirnov, M.D. Scanlon, D. Momotenko, H. Vrubel, M.A. Méndez, P.-F. Brevet, H.H. Girault, Gold Metal Liquid-Like Droplets, ACS Nano. 8 (2014) 9471–9481. https://doi.org/10.1021/nn503644v.

[24] E. Smirnov, P. Peljo, M.D. Scanlon, F. Gumy, H.H. Girault, Self-healing gold mirrors and filters at liquid–liquid interfaces, Nanoscale. 8 (2016) 7723–7737. https://doi.org/10.1039/C6NR00371K.

[25] M.F. Suárez-Herrera, A. Gamero-Quijano, J. Solla-Gullón, M.D. Scanlon, Mimicking the microbial oxidation of elemental sulfur with a biphasic electrochemical cell, Electrochim. Acta. 401 (2022) 139443. https://doi.org/10.1016/j.electacta.2021.139443.

[26] M.D. Scanlon, P. Peljo, L. Rivier, H. Vrubel, H.H. Girault, Mediated water electrolysis in biphasic systems, Phys. Chem. Chem. Phys. 19 (2017) 22700–22710. https://doi.org/10.1039/c7cp04601d.

[27] M.D. Scanlon, P. Peljo, M.A. Méndez, E. Smirnov, H.H. Girault, Charging and discharging at the nanoscale: Fermi level equilibration of metallic nanoparticles, Chem. Sci. 6 (2015) 2705–2720. https://doi.org/10.1039/c5sc00461f.

[28] P.S. Toth, Q.M. Ramasse, M. Velický, R.A.W. Dryfe, Functionalization of graphene at the organic/water interface, Chem. Sci. 6 (2015) 1316–1323. https://doi.org/10.1039/C4SC03504F.

[29] E.J.G. Santos, E. Kaxiras, Electric-field dependence of the effective dielectric constant in graphene, Nano Lett. 13 (2013) 898–902. https://doi.org/10.1021/nl303611v.

[30] K.J. Powell, P.L. Brown, R.H. Byrne, T. Gajda, G. Hefter, S. Sjöberg, H. Wanner, Chemical speciation of environmentally significant heavy metals with inorganic ligands part 1: The Hg2+- Cl-, OH-, CO32-, so42-, and PO 43- aqueous systems (IUPAC technical report), Pure Appl. Chem. 77 (2005) 739–800. https://doi.org/10.1351/pac200577040739.

[31] M.F. Suárez-Herrera, M. Costa-Figueiredo, J.M. Feliu, Electrochemical and electrocatalytic properties of thin films of poly(3,4-ethylenedioxythiophene) grown on basal plane platinum electrodes, Phys. Chem. Chem. Phys. 14 (2012) 14391–14399. https://doi.org/10.1039/c2cp42719b.

[32] Y. Xu, M. Mavrikakis, Adsorption and dissociation of O2 on gold surfaces: Effect of steps and strain, J. Phys. Chem. B. 107 (2003) 9298–9307. https://doi.org/10.1021/jp034380x.

[33] A. Corma, H. Garcia, Supported gold nanoparticles as catalysts for organic reactions, Chem. Soc. Rev. 37 (2008) 2096–2126. https://doi.org/10.1039/b707314n.

[34] T. Fujita, P. Guan, K. McKenna, X. Lang, A. Hirata, L. Zhang, T. Tokunaga, S. Arai, Y. Yamamoto, N. Tanaka, Y. Ishikawa, N. Asao, Y. Yamamoto, J. Erlebacher, M. Chen, Atomic origins of the high catalytic activity of nanoporous gold, Nat. Mater. 11 (2012) 775–780. https://doi.org/10.1038/nmat3391.

[35] M.S. Ide, R.J. Davis, The important role of hydroxyl on oxidation catalysis by gold nanoparticles, Acc. Chem. Res. 47 (2014) 825–833. https://doi.org/10.1021/ar4001907.

[36] N. Younan, M. Hojeij, L. Ribeaucourt, H.H. Girault, Electrochemical properties of gold nanoparticles assembly at polarised liquid|liquid interfaces, Electrochem. Commun. 12 (2010) 912–915. https://doi.org/10.1016/j.elecom.2010.04.019.

[37] Z. Shi, J. Lipkowski, Chloride adsorption at the Au(111) electrode surface, J. Electroanal. Chem. 403 (1996) 225–239. https://doi.org/10.1016/0022-0728(95)04313-

6.

[38] A. Sanchez, S. Abbet, U. Heiz, W.D. Schneider, H. Häkkinen, R.N. Barnett, U. Landman, When Gold Is Not Noble: Nanoscale Gold Catalysts, J. Phys. Chem. A. 103 (1999) 9573–9578. https://doi.org/10.1021/jp9935992.

[39] Y.F. Huang, M. Zhang, L. Bin Zhao, J.M. Feng, D.Y. Wu, B. Ren, Z.Q. Tian, Activation of oxygen on gold and silver nanoparticles assisted by surface plasmon resonances, Angew. Chemie - Int. Ed. 53 (2014) 2353–2357. https://doi.org/10.1002/anie.201310097.

[40] M.F. Suárez-Herrera, M.D. Scanlon, On the non-ideal behaviour of polarised liquid-liquid interfaces, Electrochim. Acta. 328 (2019) 135110. https://doi.org/10.1016/j.electacta.2019.135110.

[41] V.T. Joy, T.K.K. Srinivasan, Ft-SERS studies on 1,3-thiazolidine-2-thione, 2,5-dimercapto-1,3,4-thiadiazole and 2-thiouracil adsorbed on chemically deposited silver films, J. Raman Spectrosc. 32 (2001) 785–793. https://doi.org/10.1002/jrs.748.

[42] M. Tiwari, S. Gupta, R. Prakash, One pot synthesis of coordination polymer 2,5-dimercapto-1,3,4-thiadiazole–gold and its application in voltammetric sensing of resorcinol, RSC Adv. 4 (2014) 25675–25682. https://doi.org/10.1039/C4RA02983F.